Brief Papers

The Effects of a Ground Shield on the Characteristics and Performance of Spiral Inductors

Seong-Mo Yim, Tong Chen, and Kenneth K. O

***Abstract*—The frequency dependence of the model parameters of patterned ground shield (PGS) inductors in large part is explained as a consequence of modeling a distributed system with a lumped model. The effects of PGS shape and material on inductor characteristics have been examined and explained. There is an optimum area for a PGS to maximize Q. Using an n^+ buried/n-well PGS, the peak Q is improved by $\sim$25% from that of an inductor without a PGS while only slightly changing L and C_p in comparison to inductors with other PGSs. Having a PGS does not significantly improve isolation between adjacent inductors when isolation is limited by magnetic coupling since a PGS is specifically designed to limit termination of magnetic fields.**

***Index Terms*—Distributed system, frequency dependence, isolation, spiral inductor.**

I. Introduction

An ON-CHIP spiral inductor is one of the critical components for implementing radio-frequency integrated circuits such as a low-noise amplifier, a voltage-controlled oscillator, and an impedance matching network [1]–[3]. One of the most important parameters of spiral inductors is the quality factor Q, which is mainly limited by the loss due to inductor metal resistance, substrate resistance, and that associated with induced eddy current below the inductor metal trace [4].

Focusing on the effects of $R_{\rm sub}$, when $R_{\rm sub}$ in the commonly used equivalent circuit model shown in Fig. 1(b) is increased to infinity, the current through $R_{\rm sub}$ becomes zero, and power dissipation in $R_{\rm sub}$ becomes zero and Q is increased. When $R_{\rm sub}$ is decreased to zero, power dissipation in $R_{\rm sub}$ becomes zero again, and Q is increased [5]. The use of a patterned ground shield (PGS) between inductor metal trace and substrate increases Q [6], [7] by reducing $R_{\rm sub}$ while not inducing significant eddy current which can significantly reduce Q. The patterned sections of a shield are tied together using a metal connection. It is important to make sure that a loop is not formed in this metal connection.

In this paper, the effects of ground shield shape and material which can be formed in a silicon bipolar process are reported. The extracted inductance model parameter L, shown in Fig. 1(d), exhibits a stronger frequency dependence for PGS inductors. This frequency dependence of L and the frequency dependence of the series resistance model parameter R_S are explained as a consequence of modeling a distributed system using a lumped element model. Additionally, contrary to a previous report [6], it is shown that isolation characteristics between adjacent inductors are not significantly improved by the addition of a PGS, when isolation is limited by magnetic coupling [5].

Manuscript received January 12, 2001; revised October 5, 2001. This work was supported by a grant from Conexant Systems.

The authors are with the Department of Electrical and Computer Engineering, Silicon Microwave Integrated Circuits and Systems Research Group, University of Florida, Gainesville, FL 32611 USA (e-mail: smyim@tec.ufl.edu).

Publisher Item Identifier S 0018-9200(02)00668-6.

II. Experiment

Fig. 1(a) shows the 3.25-turn 4.8-nH inductor structure mostly used in this study. The metal width and space are 10 and 6 μm. The metal thickness is 3.0 μm and separated from a 20-Ω-cm substrate by $\sim$3.0 μm. The outer dimension of the inductor is 250 μm $\times$ 250 μm. Under this inductor structure, a wide variety of patterned ground shields with varying shapes and formed with metal 1, silicided polysilicon, and n^+ buried layer has been placed, and its impact has been investigated. The model parameters of the inductors extracted from measurements are listed in Table I.

III. Characteristics of Inductors

Fig. 1(a) also shows the control inductor (N9) without a PGS, N10 and N12 inductors with a four-piece poly-PGS and an eight-piece poly-PGS which has larger gaps or a reduced PGS area. Fig. 1(c)–(g) shows $Q_{\rm bw}$ [8] and the extracted model parameters for the inductors. Adding the PGS improves the peak $Q_{\rm bw}$ by $\sim$25%. The $R_{\rm sub}$ of N10 and N12 are 11 and 7 Ω, respectively, while that for the control inductor is 55 Ω. Another prominent difference between the control and PGS inductors is that inductance of the PGS inductors decreases faster with frequency. Over 4 GHz, the L of N10 and N12 is decreased by $\sim$17% versus 12% for the control. On the other hand, R_s of the control inductor changes more rapidly with frequency and becomes negative at high frequencies. To explain these sometime seemingly nonphysical results, the impact of modeling a distributed system using the simple lumped model is investigated.

IV. Distributed Model of Inductors

A spiral inductor is a type of transmission lines [9]–[11] and can be modeled as sections of magnetically coupled transmission

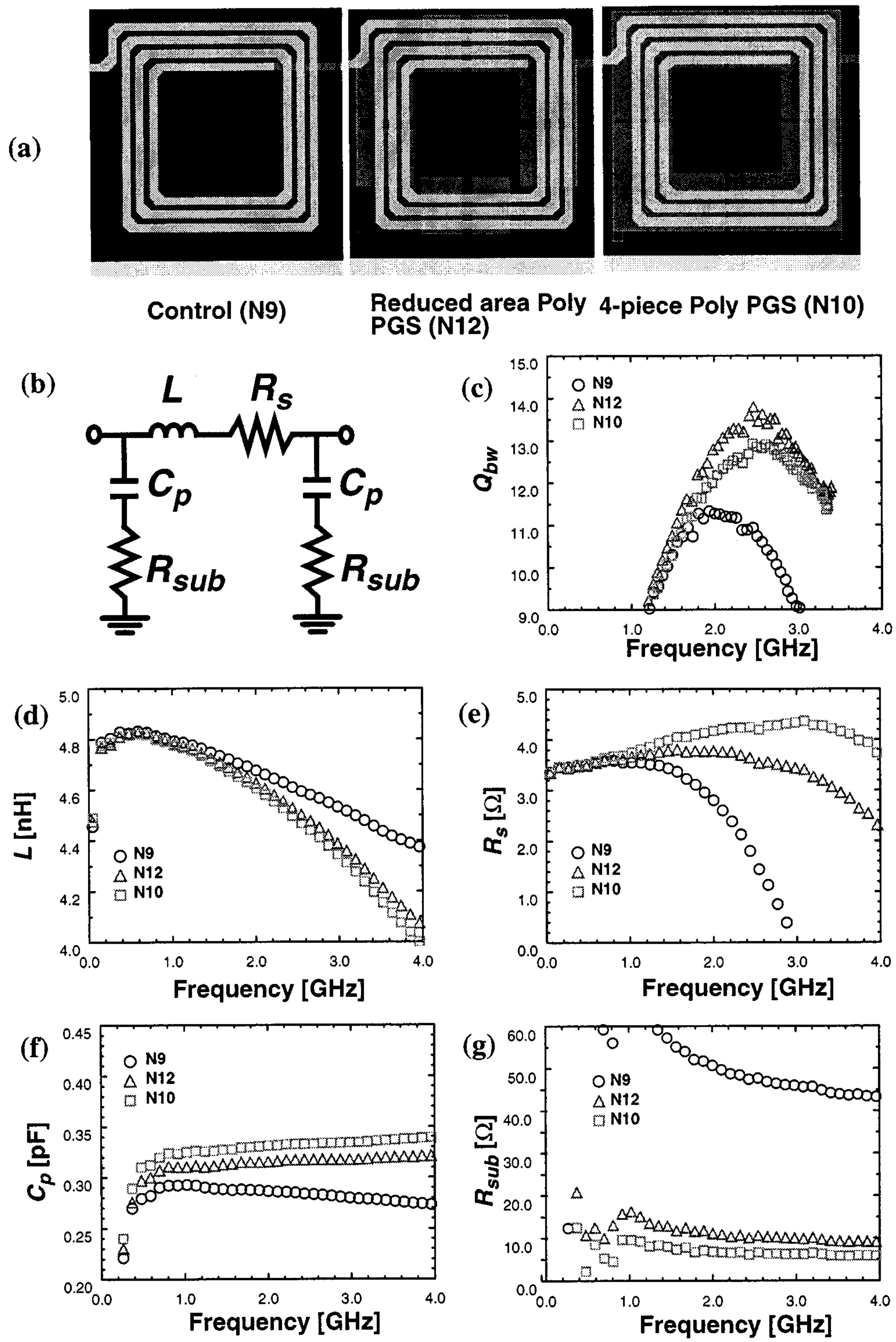

Fig. 1. (a) Inductors with a different ground shield area. (b) Commonly used equivalent circuit model for an inductor. (c) $Q_{\rm bw}$. (d) L. (e) R_s. (f) C_p. (g) $R_{\rm sub}$ versus frequency.

lines. In reality, the substrate eddy current effect, skin effect, proximity effect, their associated distributed effects, and others should also be included. These make physics-based modeling of spiral inductors difficult. As a first-order attempt to study the impact of modeling a distributed system using a simple lumped element model shown in Fig. 1(b), model parameters for a section of a distributed N-section model have been generated by scaling down L and R_s by N, and C_p by $(N+1)/2$, and by scaling up $R_{\rm sub}$ by $(N+1)/2$ [Fig. 2(a)]. When $N=1$, these distributed model parameters are the same as the lumped model parameters. In real spiral inductors, the inductors are not symmetric and these sections are not equally distributed. Therefore, the model parameters of these sections are not necessarily the same. However, for the purpose of

TABLE I
MEASURED PARAMETERS OF SPIRAL INDUCTORS

	N9	N10	N12	N17	N5	N6	N15	M1	M2	M3
L [nH]	4.8	4.8	4.8	4.8	4.8	4.8	4.8	5.3	5.3	5.3
R_s [Ω]	3.3	3.3	3.3	3.3	3.3	3.3	3.3	18.5	18.5	18.5
C_p [fF]	290	325	310	340	330	300	420	950	380	320
R_{sub} [Ω]	55	11	7	6	7	9	6	6	6	6
Q_{bw} @max.	11.3	12.9	13.8	13.9	14.3	13.5	11.5	---	---	---

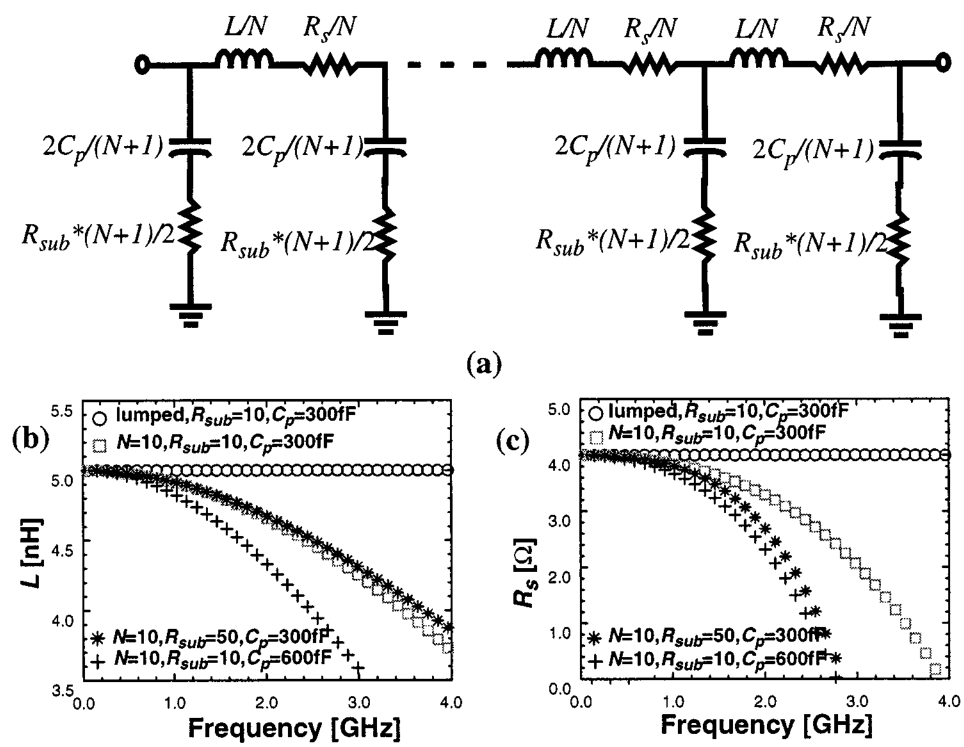

Fig. 2. (a) Distributed line model. (b) Re-extracted L. (c) Re-extracted R_s when the original lumped R_s and L are 4.2 Ω and 5.1 nH.

examining the impact of modeling a distributed system using a lumped model, this approximation should be acceptable. Treating this distributed model as a lumped system, L and R_s are re-extracted and shown in Fig. 2(b) and (c). At low frequencies, as it should be, the extracted L and R_s are the same for both cases. However, when a distributed system is treated as a lumped system, extracted L and R_s decrease with frequency like the measured results shown in Fig. 1. The number of sections was ten. It was found that increasing the number beyond ten had small effects on the re-extracted model parameters for the inductors used in this study. In general, the number of sections N should be chosen that the percentage (%) error (1) should be small.

$$\%\ \text{error} = \frac{\coth(\gamma\cdot x) - (N+1)\cdot\frac{\alpha^{2N+1}+\beta^{2N+1}}{\alpha^{2N+2}-\beta^{2N+2}}}{\coth(\gamma\cdot x)}\times 100. \quad (1)$$

In this expression, x is the length of a spiral inductor, and ω is the frequency in radian. $\gamma\cdot x$ is expressed in (2), shown at the bottom of the next page. α and β in (1) are

$$\alpha = \sqrt{N\cdot(N+1)+\left(\gamma\cdot\frac{x}{2}\right)^2}+\left(\gamma\cdot\frac{x}{2}\right)$$
$$\beta = \sqrt{N\cdot(N+1)+\left(\gamma\cdot\frac{x}{2}\right)^2}-\left(\gamma\cdot\frac{x}{2}\right).$$

For this study, inductors with $R_{\rm sub}$ of 10 and 50 Ω, and C_p [Fig. 1(b)] of 300 and 600 fF are evaluated. The frequency dependence of L increases as $R_{\rm sub}$ is decreased and as C_p is increased, though the dependence on $R_{\rm sub}$ is weaker. As seen in Fig. 1, C_p of the PGS inductors is larger than that of the control inductor (N9) while $R_{\rm sub}$ is significantly lower. These can easily explain the stronger frequency dependence of L for the PGS inductors. The re-extracted R_s decreases faster with frequency if $R_{\rm sub}$ and C_p are increased, and it can become negative. These

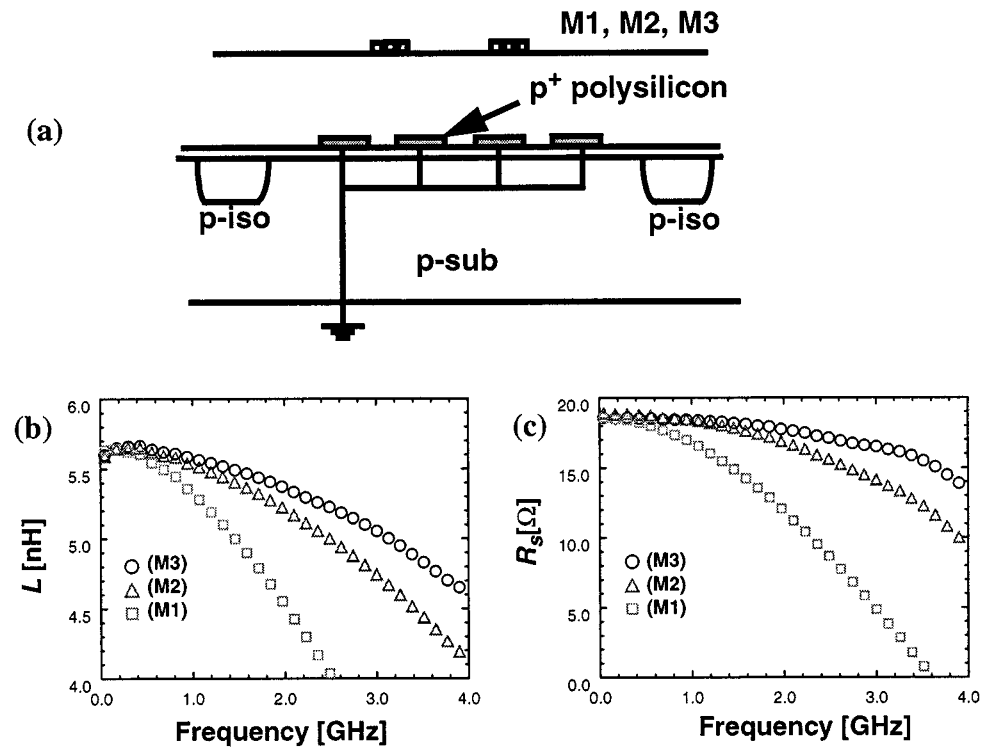

Fig. 3. (a) Inductors formed with a metal-1, metal-2, or metal-3 while using the same polysilicon PGS. (b) L. (c) R_s versus frequency.

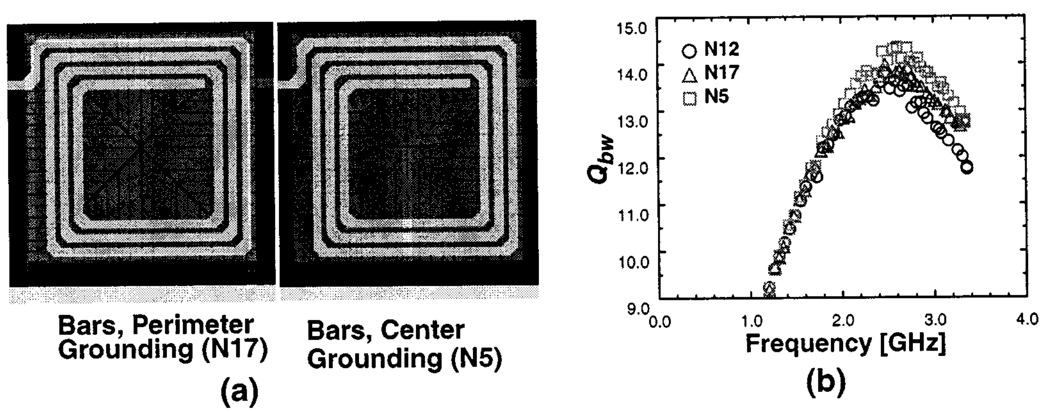

Fig. 4. (a) Inductors with a reduced area poly PGS and with a different current collecting method. (b) $Q_{\rm bw}$ versus frequency.

can once again explain the measured behaviors of R_s shown in Fig. 1(e). For the inductors considered in this investigation, doubling C_p from 300 fF has the same effect as increasing $R_{\rm sub}$ by a factor of 5 from 10 Ω. For N10 and N12 inductors, when the PGSs are added, $R_{\rm sub}$ decreases by almost a factor of 5, while at the maximum, C_p increases by $\sim$20%. Because of this, the $R_{\rm sub}$ effect dominates and the frequency dependence of R_s decreases when a PGS is added.

These also explain the stronger frequency dependence of L and R_s for an inductor fabricated with the metal-1 layer on a polysilicon PGS with higher C_p compared to those fabricated with the metal-2 and metal-3 layer using the same polysilicon PGS (Fig. 3). As the separation between the PGS and inductor metal trace is decreased, C_p is increased, thus the frequency dependence of L and R_s is increased. These effects of modeling a distributed system with a lumped model, however, cannot ex-

$$\gamma \cdot x = \sqrt{(R_s + j\omega L) \cdot \left(\frac{2 \cdot \omega^2 \cdot C_p^2 \cdot R_{\rm sub}}{1 + \omega^2 \cdot C_p^2 \cdot R_{\rm sub}^2} + j\omega \cdot \frac{2 \cdot C_p}{1 + \omega^2 \cdot C_p^2 \cdot R_{\rm sub}^2} \right)} \quad (2)$$

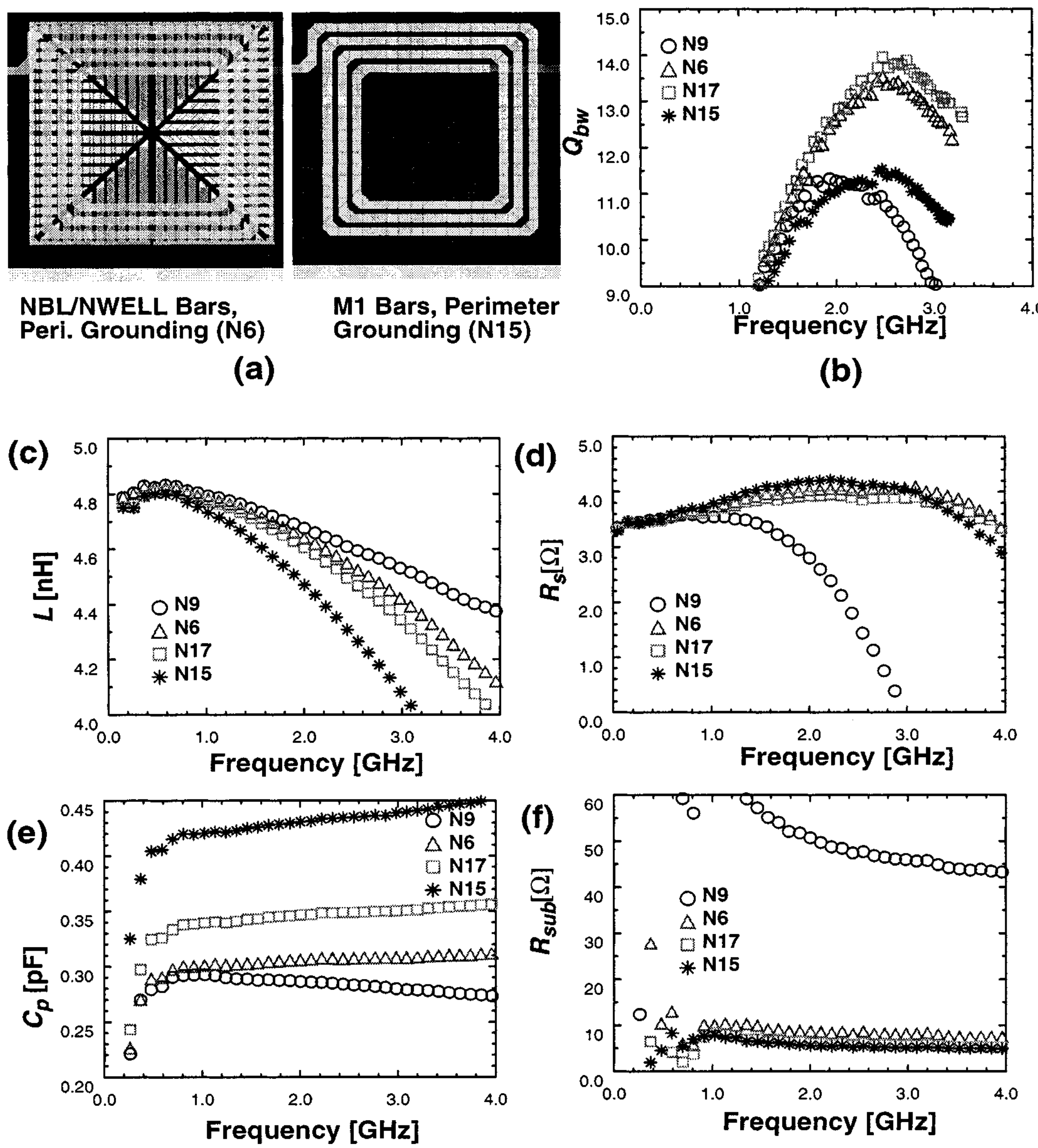

Fig. 5. (a) Inductors with a different ground shield area. (b) $Q_{\rm bw}$. (c) L. (d) R_s. (e) C_p. (f) $R_{\rm sub}$ versus frequency.

plain the increase in R_s for PGS inductors with frequency at lower frequencies seen in Fig. 1(e). This is typically attributed to the skin effect and eddy current loss, which have not been included in the models.

V. Effects of Ground Shield Shape

Referring back to Fig. 1, the Q of the N12 inductor (with a reduced PGS ground shield area) is slightly higher (around 1) than that for N10 with a four-piece PGS. The C_p of N12 is decreased by $\sim 5\%$ ($\sim$15 fF) from that for N10. The fact that the PGS area of N12 is around 60% of that of N10 increases $R_{\rm sub}$ of N12 to 11 Ω from 7 Ω. The net effect of these was to make N12 have slightly lower frequency dependent L and slightly higher frequency dependent R_s than that for N10. Based on these, it is clear that the PGS shape also affect the frequency dependence of L and R_s.

At moderate to high frequencies, R_s of N12 is lower than that for N10. This explains the slightly higher peak Q for N12. Despite the fact that R_s of N9 is lower, because of the higher $R_{\rm sub}$, the peak Q is lower for N9. Therefore, the reduced area inductor (N12) has the highest Q among N9, N12, and N10. If the area of PGS is reduced too much, $R_{\rm sub}$ will eventually become too high and Q should decrease. As seen for the control inductor with a zero PGS area, because of its highest $R_{\rm sub}$, it has the lowest Q among the three inductors. These mean there must be an optimum area for PGS to maximize Q. Among the three, N12 is the best design.

Fig. 4 compares Q of inductors with a PGS shape from [6] (N17) to that of N12. Additionally, a PGS structure in which the PGS ground current is extracted from the center has been evaluated (N5). Since the ground current can be significant, there can be nonnegligible magnetic energy storage and inductance associated with the connections for extracting the current. N5

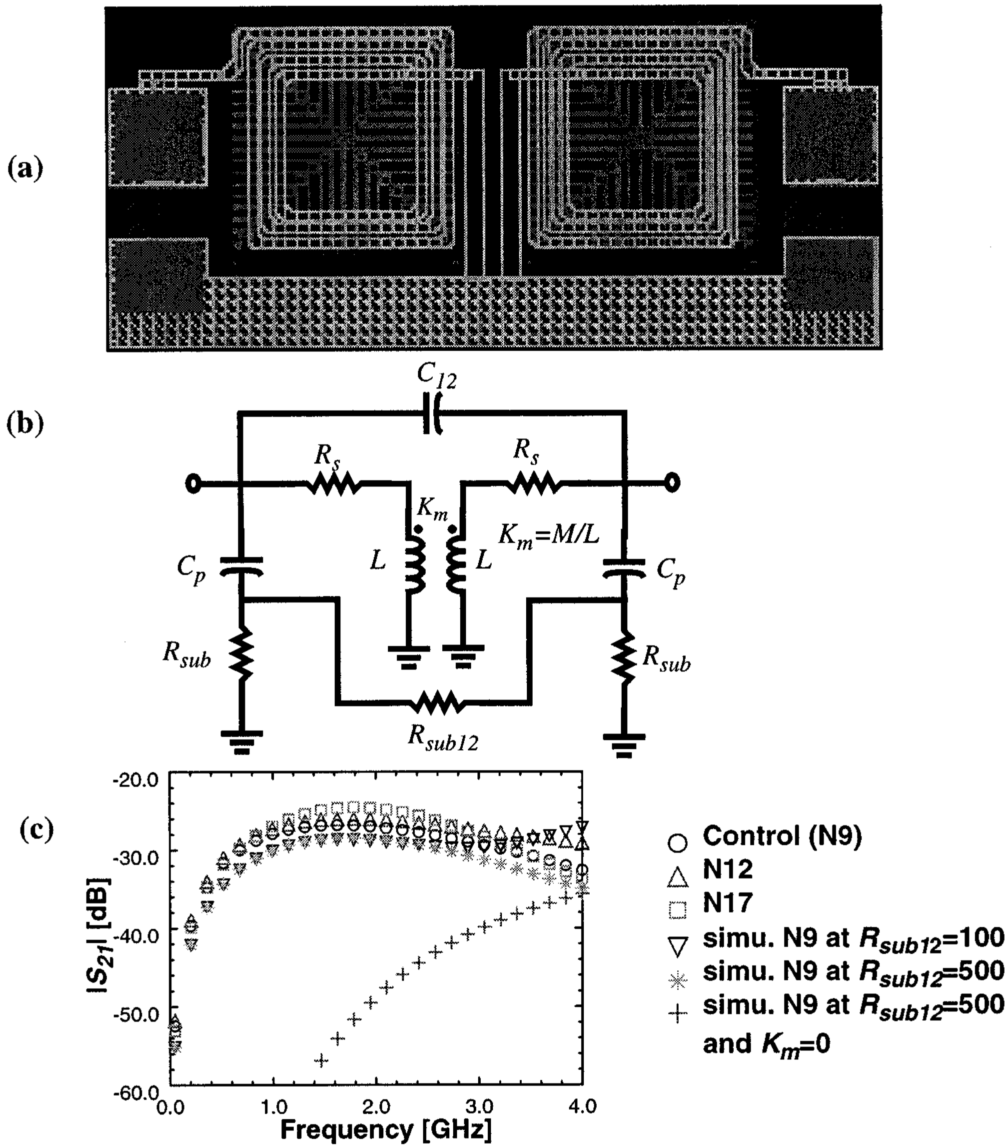

Fig. 6. (a) Inductor isolation test structure. (b) Lumped equivalent circuit model for the isolation test structure. (c) Measured $|S_{21}|$ for the isolation structures using N9, N12, N17, and simulated $|S_{21}|$ for the structure using N12 at $R_{\rm sub12} = 100,\ 500\ \Omega$ and for that using N9 at $R_{\rm sub12} = 500\ \Omega$ with $K_m = 0$.

and N17 have a poly-PGS with 11.6-μm-wide bars separated by 1.6 μm. The peak Q of N5 is slightly higher than that of N12 and N17. Although the differences are small, N5 has the highest Q among the inductors with varying PGS shapes considered in this study.

VI. Effects of Ground Shield Materials

Fig. 5 shows an inductor with a PGS formed using an n$^+$ buried layer (nbl) and an n-well layer (N6), and another inductor with a metal-1 PGS (N15). The sheet resistance of the buried layer is ~25 $\Omega/\square$. The width and space of the nbl shields are 8 and 4 μm, respectively. The width and space of the bars for the metal-1 PGS (N15) are 11.6 and 1.6 μm, respectively. C_p's of N6 and N17 are ~5 and ~25% higher than that for the control inductor (N9). C_p of N15 is the highest and around 1.6 times C_p for N9. Among N6, N17, and N15, the frequency dependence of L is the weakest for N6 which has the largest separation between the inductor metal trace and PGS or the lowest C_p. The frequency dependence is the highest for N15 which has the smallest separation or the highest C_p. This is once again consistent with the earlier discussion on frequency dependence of L resulting from modeling a distributed system with a lumped model. N17 has slightly higher peak Q than N6. N15, however, has the lowest $R_{\rm sub}$, because its inductance decreases more rapidly with frequency due to higher C_p, the peak Q for N15 is significantly lower than that for N6 and N17. In this bipolar process, by using a PGS with an n$^+$ buried/n-well layer combination, it is possible to improve the peak Q by ~25% with small changes in the characteristics of C_p and L. If a larger C_p can be tolerated, the peak Q can be improved slightly more by using a polysilicon PGS.

VII. Isolation Between Adjacent Inductors

It has been suggested that having a PGS can improve isolation between adjacent inductors by ~30 dB [6]. To investigate the dependence of isolation on the PGS shape, test structures have been implemented. Fig. 6(a) shows an isolation structure formed with N17. One of the terminals of each inductor is grounded. The second terminal of each inductor is connected to pads and S_{21} between these two pads are measured. The inductors are separated by ~85 μm. The structure like this can be found in a differential *LC*-tuned voltage-controlled oscillator (VCO). Fig. 6(c) shows $|S_{21}|$ of the isolation structures. Contrary to the previous report [6], the isolation characteristics are not significantly affected by the presence of a PGS and PGS shape. The PGS by design does not significantly perturb the magnetic field generated by the inductor. This means that if the signal coupling between the two inductors is magnetic in nature, then isolation characteristics should not be significantly affected by the presence of a PGS.

To study this, an equivalent circuit model for the isolation structure is constructed and shown in Fig. 6(b). Fig. 6(c) also shows simulated isolation characteristics with and without including the magnetic coupling [$K_m = M/L =$ 0.037; see Fig. 6(b)]. In addition to the inductor model parameters discussed earlier, $R_{\rm sub12}$ and C_{12} are included to model signal coupling between the two control inductors (N9) through substrate and the capacitance between two inductors, respectively. C_{12} and its impact are usually small. The model values were $L =$ 4.8 nH, $R_s =$ 3.6 Ω, $C_p =$ 300 fF, $R_{\rm sub} =$ 50 Ω, which are comparable to those of the control inductor. The coupling coefficient, K_m was computed using the layout and Greenhouse formula [12]. The simulated isolation degrades by ~20 dB or more at 1.8 GHz, when the magnetic coupling is included.

Fig. 6(c) also shows the dependence of $|S_{21}|$ on $R_{\rm sub12}$ (100, or 500 Ω). When $R_{\rm sub} =$ 50 Ω, which is close to that for the control inductor, if $R_{\rm sub12}$ is much greater than 100 Ω, it does not affect $|S_{21}|$. Between 3 and 4 GHz, when $R_{\rm sub12}$ (100 Ω) is comparable to $R_{\rm sub}$, $|S_{21}|$ increases with frequency. The fact that this rise of $|S_{21}|$ is not seen in the measurements suggests that the $R_{\rm sub12}$ is larger than 100 Ω for the control inductor. The impact of $R_{\rm sub12}$ is more complicated for PGS inductors because of the presence of an oxide layer between the PGS and substrate. At the same time, the $R_{\rm sub12}$ effect should be smaller, since $R_{\rm sub}$ is much smaller and the oxide layer increases the impedance and reduces the substrate coupling.

If the effects of coupling through $R_{\rm sub12}$ and C_{12} are neglected (i.e., $R_s = 0$, $R_{\rm sub} = 0$, $L \gg M$, and $C_{12} = 0$), then the transducer gain or $|S_{21}|^2$ can be estimated as shown in the equation at the bottom of the page, where Z_O is the 50-Ω characteristic impedance. When the frequency goes to 0 and when it becomes high, the expression is reduced to

$$\text{As } \omega \to 0 \text{ Hz}, \ |S_{21}| \approx \frac{2 \cdot M}{Z_O} \cdot \omega$$

$$\text{As } \omega \to \text{high}, \ |S_{21}| \approx \frac{2 \cdot M}{Z_O} \cdot \left(\frac{1}{L \cdot C_p}\right)^2 \cdot \left(\frac{1}{\omega}\right)^3.$$

At low frequencies, as frequency is increased, the coupling increases linearly because of the mutual inductance effect, while at high frequencies, the coupling decreases with frequency because C_p at the port 2 shunts the port to ground. These result in a peak as seen in the measured $|S_{21}|$ plots. The difference between the simulated and the measured $|S_{21}|$ is around 2 dB for the control inductor, which is a good agreement given that all the frequency dependence of the model parameters are neglected. These indeed suggest that isolation is limited by the magnetic coupling and in this limit, having a PGS does not significantly improve isolation between two adjacent inductors.

VIII. Conclusion

The frequency dependence of the model parameters for 3.25-turn 4.8-nH PGS spiral inductors can be largely explained as a consequence of modeling a distributed system using a lumped model. If a distributed system is treated as a lumped system, re-extracted L and R_s decrease as frequency increases. The frequency dependency of L increases as C_p is increased and decreases a little as $R_{\rm sub}$ is increased. The frequency dependency of R_s increases if C_p and $R_{\rm sub}$ are increased. PGS inductors have higher frequency dependency of L and lower frequency dependency of R_s than the control inductors because of their higher C_p and lower $R_{\rm sub}$. Due to these, Q of PGS inductors is strongly influenced by its distributed nature, and this should be factored in during the design process in order to increase Q. Additionally, there is an optimum area for PGS to maximize Q. Because the connections for ground current extraction can carry significant current, the magnetic energy storage and inductance associated with the ground connection cannot be neglected in designing inductors with a PGS. In the bipolar process utilized for this study, using a PGS formed with an n^+ buried/n-well layer combination, it is possible to improve the peak Q by ~25% with small changes in the characteristics of C_p and L. Isolation between two adjacent inductors separated by ~85 μm is limited by magnetic coupling and in this limit, having a PGS does not significantly improve isolation.

$$|S_{21}|^2 \approx \frac{(2 \cdot \omega \cdot M \cdot Z_O)^2}{\left\{\omega^4 \cdot L^2 \cdot C_p^2 \cdot Z_O^2 - \omega^2 \cdot (L^2 - 2 \cdot L \cdot C_p \cdot Z_O^2) + Z_o^2\right\}^2 + (2 \cdot \omega \cdot L \cdot Z_O)^2 \cdot \left\{\omega^2 \cdot L \cdot C_p - 1\right\}^2}$$

ACKNOWLEDGMENT

The authors are grateful to Dr. J. Zheng, P. N. Sherman, and P. Kempf of Conexant Systems for their help.

REFERENCES

[1] Y.-C. Ho, K.-H. Kim, B. A. Floyd, C. Wann, Y. Taur, I. Lagnado, and K. K. O, "4- and 13-GHz tuned amplifiers implemented in a 0.1-μm CMOS technology on SOI, SOS, and bulk substrates," *IEEE J. Solid-State Circuits*, vol. 33, pp. 2066–2073, Dec. 1998.

[2] C.-M. Hung and K. K. O, "A 1.24-GHz monolithic CMOS VCO with phase noise of -137 dBc/Hz at a 3-MHz offset," *IEEE Microwave and Guided Wave Lett.*, vol. 9, pp. 111–113, Mar. 1999.

[3] A. Hajimiri and T. H. Lee, "Design issues in CMOS differential LC oscillators," *IEEE J. Solid-State Circuits*, vol. 34, pp. 717–724, May 1999.

[4] B. Razavi, "Challenges in the design of frequency synthesizers for wireless applications," in *Proc. CICC*, May 1997, pp. 395–402.

[5] S.-M. Yim, T. Chen, and K. K. O, "The effects of a ground shield on spiral inductors fabricated in a silicon bipolar technology," in *Proc. Bipolar/BiCMOS Circuits and Technology Meeting (BCTM)*, Sept. 2000, pp. 157–160.

[6] C. P. Yue and S. S. Wong, "On-chip spiral inductors with patterned ground shields for SI-based RF ICs," *IEEE J. Solid-State Circuits*, vol. 33, pp. 734–752, May 1998.

[7] T. Chen, K. Kim, and K. K. O, "Application of a new circuit design oriented Q extraction technique to inductors in silicon IC's," in *IEDM Tech. Dig.*, 1998, pp. 527–530.

[8] K. K. O, "Estimation methods for quality factors of inductors fabricated in silicon integrated circuit process technologies," *IEEE J. Solid-State Circuits*, vol. 33, pp. 1249–1252, Aug. 1998.

[9] J. R. Long and M. A. Copeland, "The modeling, characterization, and design of monolithic inductors for silicon RF IC's," *IEEE J. Solid-State Circuits*, vol. 32, pp. 357–369, Mar. 1997.

[10] Y. Eo and W. R. Eisenstadt, "High-Speed VLSI interconnect modeling based on S-parameter measurements," *IEEE Trans. Comp., Hybrids, Manufact. Technol.*, vol. 16, pp. 555–562, Aug. 1993.

[11] R. Groves, D. L. Harame, and D. Jadus, "Temperature dependence of Q and inductance in spiral inductors fabricated in a silicon-germanium/BiCMOS technology," *IEEE J. Solid-State Circuits*, vol. 32, pp. 1455–1459, Sept. 1997.

[12] H. M. Greenhouse, "Design of planar rectangular microelectronic inductors," *IEEE Trans. Parts, Hybrids, Packag.*, vol. PHP-10, pp. 101–109, June 1974.